Local electronic and crystal structure of rare-earth cobalt phosphides RCo_2P_2 (R = La, Ce, Pr, Nd, Eu) studied by XAFS and RIXS

2013 J. Phys.: Conf. Ser. 430 012105

(http://iopscience.iop.org/1742-6596/430/1/012105)

Journal of Physics: Conference Series **430** (2013) 012105 doi:10.1088/1742-6596/430/1/012105

Local electronic and crystal structure of rare-earth cobalt phosphides RCo_2P_2 (R = La, Ce, Pr, Nd, Eu) studied by XAFS and RIXS

A A Yaroslavtsev[1], A P Menushenkov[1], I A Zaluzhnyy[1], R V Chernikov[2], W Caliebe[2], C M Thompson[3], A A Arico[3], K Kovnir[4] and M Shatruk[3]

[1] National Research Nuclear University "MEPhI", Kashirskoe sh., 31, Moscow 115409, Russia
[2] HASYLAB at DESY, Notkestrasse, 85, Hamburg D-22607, Germany
[3] Department of Chemistry and Biochemistry, Florida State University, Chieftan Way, 95, Tallahassee, FL 32306, USA
[4] Department of Chemistry, University of California at Davis, One Shields Avenue, Davis, CA 95616, USA

E-mail: yalex03@gmail.com

Abstract. A detailed combined study of local electronic and crystal structures was performed for a series of rare-earth cobalt phosphides RCo_2P_2 (R = La, Ce, Pr, Nd, Eu) with peculiar itinerant magnetic ordering schemes using different methods employing the synchrotron radiation: RIXS, XANES and EXAFS. Europium and cerium are shown to be in the intermediate valence state in all compounds. The correlation between rare-earth valence and the observed changes of magnetic ordering in the systems under investigation is discussed.

1. Introduction

The rare-earth cobalt phosphides RCo_2P_2 (R = La, Ce, Pr, Nd, Eu) with the $ThCr_2Si_2$-type crystal structure demonstrate multiple transitions between states with the different ordering of magnetic moments in the sublattices of $4f$ rare-earth elements and $3d$ transition metals. In these materials the magnetic properties are dictated by peculiarities of electronic band structure at the Fermi level, which can be affected by external perturbation, e.g. pressure [1]. The similar modification of electronic structure can be induced by chemical compression via non-isoelectronic substitution in the rare-earth sublattice. While the pure $EuCo_2P_2$ is antiferromagnetic with magnetic Eu($4f$)-sublattice (T_N = 66.5) K, the $Pr_{0.8}Eu_{0.2}Co_2P_2$ compound is unexpectedly ferromagnetic (T_C = 282 K) with magnetic Co($3d$)-sublattice [2]. In the series $La_{1-x}R_xCo_2P_2$ the Ce-substituted phases behave quite differently from the Pr- and Nd-substituted ones [3]. Therefore, the motivation of this work was to use the local-sensitive methods of resonant inelastic X-ray scattering (RIXS) and the X-ray absorption fine structure (XAFS) spectroscopy to explore in detail the features of local electronic and crystal structure of RCo_2P_2, in particular the possible intermediate valence state of Eu and Ce.

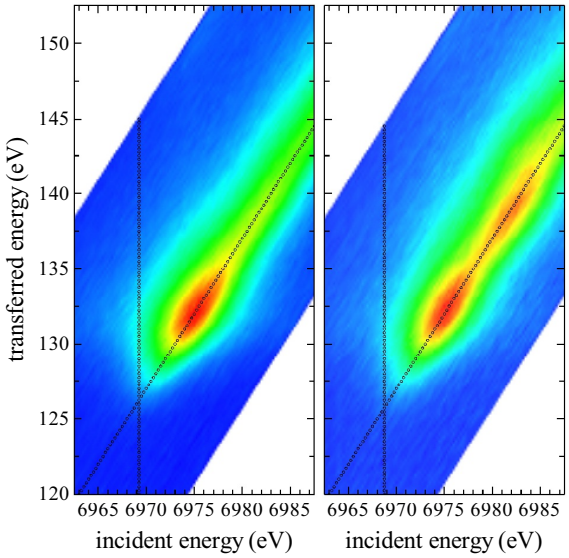

Figure 1. RIXS maps of $EuCo_2P_2$ (left) and $Nd_{0.6}Eu_{0.4}Co_2P_2$ (right). The maximum of Eu $L\beta_{2,15}$ fluorescence intensity is marked with a diagonal line. The emission spectrum at the incident photon energy $h\nu_{in}$ = 6970.7 eV is marked with a vertical line

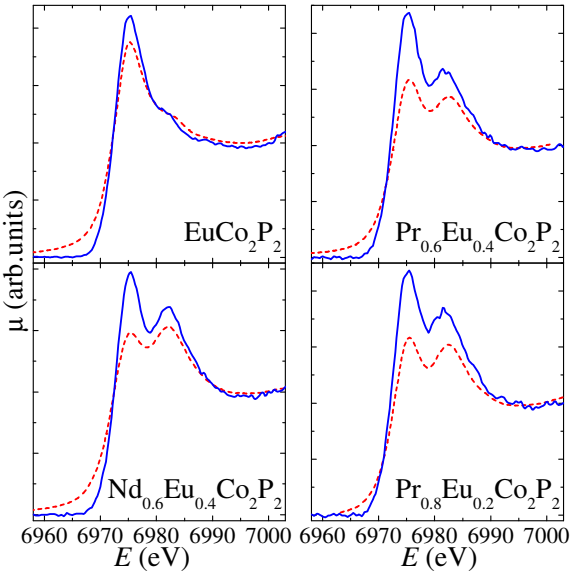

Figure 2. The comparison of high energy resolution fluorescence detected absorption (HERFD) spectra (——) at the L_3-Eu absorption edge with the XANES-spectra (- - - -) for various samples

2. Experimental

The samples $Pr_{1-x}Eu_xCo_2P_2$ (x = 0.1, 0.2, 0.3, 0.4, 1.0), $Nd_{0.6}Eu_{0.4}Co_2P_2$ and $La_{1-x}Ce_xCo_2P_2$ (x = 0.3; 0.6; 0.9) were prepared by standard procedures reported in [2, 3]. The phase purity of bulk products obtained was confrmed by powder X-ray diffraction. The full RIXS maps of $EuCo_2P_2$-based samples were collected at W1 beamline of DORIS-III storage ring (HASYLAB/DESY, Hamburg, Germany) at room temperature using the high-resolution X-ray spectrometer equipped with a spherically bent Si(531) analyzer crystal by measuring the intensity of Eu $L\beta_{2,15}$ emission line with the maximum at 6843.2 eV while scanning the incident photon energy $h\nu_{in}$ with the 0.5 eV step around the L_3-Eu absorption edge (6977 eV). The X-ray absorption spectra of all studied samples were collected at C and A1 beamlines of DORIS-III in the transmission mode above the L_3-Eu (6977 eV), L_3-Ce (5723 eV), L_3-Pr (5964 eV) and K-Co (7709 eV) absorption edges. Energy resolution of the double-crystal Si (111) monochromator at 7 keV was about 1.2 eV. Low-temperature measurements were carried out using a liquid helium continuous flow cryostat with a temperature control of ±1 K at 300 K and ±0.1 K at 5 K.

3. Results and discussion

In curent RIXS study the core-hole decay channel $2p^5 4f^N \epsilon d \rightarrow 4d^9 4f^N \epsilon d$ (Eu $L\beta_{2,15}$) was chosen. Since the $4d$ core-hole has the longer liftime than the $2p$ core-hole, the spectral broadening was reduced from $\Gamma_{2p} \sim 3.9$ eV to $\Gamma_{4d} \sim 2.75$ eV, as shown below. Besides, Eu $L\beta_{2,15}$ emission line is free from any Pr and Nd fluorescense contributions, which improves the precision of Eu valence determination.

The two-dimensional RIXS maps of samples $EuCo_2P_2$ and $Nd_{0.6}Eu_{0.4}Co_2P_2$ are shown in fig. 1. The energy transferred to the sample, i.e. $h\nu_T = h\nu_{in} - h\nu_{out}$, is shown along the vertical axis. In this plot, the emission line at constant photon energy $h\nu_{out}$ is represented by a diagonal line crossing from the lower left to the top right corner of the RIXS map. In

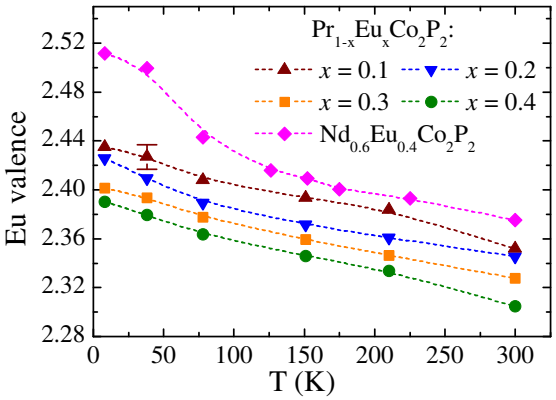

Figure 3. Temperature dependence of Eu valence in $(Pr,Nd)_{1-x}Eu_xCo_2P_2$ samples

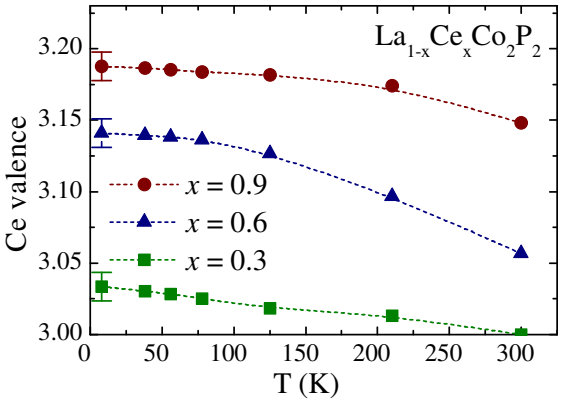

Figure 4. Temperature dependence of Ce valence in $La_{1-x}Ce_xCo_2P_2$ samples

the map of $Nd_{0.6}Eu_{0.4}Co_2P_2$ there are two pronounced resonances at $h\nu_{in,1} \sim 6975.5$ eV and $h\nu_{in,2} \sim 6975.5$ eV, corresponding to the Eu^{2+} and Eu^{3+} configurations. Both resonances are visible at single emission energy $h\nu_{out} = 6843.2$ eV, because the $2p$ and $4d$ levels are localized and equally screened by the $4f$ orbital. In the map of pure $EuCo_2P_2$, only the Eu^{2+} resonance is clearly resolved while the Eu^{3+} resonance is resolved partially. The RIXS spectra of the Pr-doped samples are similar to that of $Nd_{0.6}Eu_{0.4}Co_2P_2$. The presence of two resonances in the RIXS and XANES spectra and a single signal in the ^{151}Eu Mössbauer spectra [1, 2] indicate the intermediate valence state of europium [4]. This is due to the different timescales of Mössbauer spectroscopy (10^{-8} s) and X-ray absorption spectroscopy (10^{-15} s).

Fig. 2 shows the high energy resolution fluorescence detected absorption (HERFD) spectra, taken at a maximum of Eu $L\beta_{2,15}$ fluorescence intensity (shown with a diagonal line in fig. 1), in comparison to the transmission XANES spectra of the samples. Both series of spectra reveal a structure consisting of two maxima at $h\nu_{in,1} \sim 6975.5$ eV and $h\nu_{in,2} \sim 6982.0$ eV that correspond to the Eu^{2+} and Eu^{3+} contributions. The HERFD spectra, however, are broadened much less than the XANES-spectra, which provides an advantage in the accurate determination of the Eu^{2+} to Eu^{3+} resonance amplitude ratio. Besides, the lesser broadening reveals the absence of quadrupolar $2p \rightarrow 4f$ contribution in the pre-edge region.

In order to determine the Eu valence, the split peaks in the HERFD spectra were analyzed the same way as commonly done for XANES spectra. The processing was performed using XANES dactyloscope program [5]. The modeling of experimental spectra and the determination of $4f^7$ (Eu^{2+}) and $4f^6$ (Eu^{3+}) contributions was performed using the conventional fitting with the combination of analytical functions with constrained widths and energy positions [6] and also using the theoretical spectrum of $EuCo_2P_2$ pre-calculated with FDMNES [7] as an integer valence standart. The fitting revealed that the width of individual valence components in the HERFD spectra was ~ 2.75 eV, whereas in the XANES spectra the width varies from 3.63 to 4.08 eV for different samples. The Eu valence in the Nd-containing sample (+2.336) is larger than in the $Pr_{1-x}Eu_xCo_2P_2$ (+2.298 for $x = 0.4$ and +2.341 for $x = 0.2$). This might be explained by the smaller ionic radius of Nd^{3+} as compared to Pr^{3+}. The pure $EuCo_2P_2$ sample also exhibits an intermediate Eu valence of ~ 2.15 [8]. Although the total magnitude of absorption maxima of HERFD spectra is reduced by the self-absorption, the ratio of two valence contributions is affected insignificantly, and the relative error of final valence values is not bigger than 1%.

Since the recording of RIXS maps was very time-demanding (over 6 h for one map), the temperature dependences of Eu valence in $(Pr,Nd)_{1-x}Eu_xCo_2P_2$ and Ce valence in $La_{1-x}Ce_xCo_2P_2$ were obtained only by means of XANES. The Eu valence in $Pr_{1-x}Eu_xCo_2P_2$

increases from +2.30 in $x = 0.4$ sample at 300 K to +2.44 in $x = 0.1$ sample at 8 K (Fig. 3). The Eu valence in Nd-containing sample increases from +2.39 at 300 K to +2.51 at 8 K with the curvature in the direction of valence increase in the low temperature region, which is not observed for the Pr-doped samples. Interestingly, the valence ~ 2.15 of Eu in the pure $EuCo_2P_2$ does not change significantly upon temperature decrease. Thus, in this sample the intermediate valence state of Eu coexists with the antiferromagnetic ordering of Eu sublattice below $T_N = 66.5$ K [1]. The Ce valence in $La_{1-x}Ce_xCo_2P_2$ samples increases from integer +3.00 in $x = 0.3$ sample at 300 K to +3.19 in $x = 0.9$ sample at 8 K (Fig. 4). Notably, the discrepancy between XANES and HERFD results at room temperature is not such a significant: it does not exceed 0.04. This indicates that the common XANES spectroscopy is still precise enough in order of rare-earth intermediate valence determination if the correct fitting parameters are chosen.

The refinement of RCo_2P_2 local crystal structure by EXAFS is reported elsewhere [9]. The most important results are a split of rare-earth coordination shell around Co atom and the correlation between local R-Co and Co-Co distances and Ce valence, which are strongly related to interaction between the rare-earth $4f$ states and Co $3d$ states.

4. Conclusion

The results of RIXS and XANES spectroscopy demonstrate the intermediate valence state of Eu and Ce in all the studied RCo_2P_2 compounds, including pure $EuCo_2P_2$, despite the antiferromagnetic ordering in the Eu sublattice of the latter [1]. The cooling, Pr/Nd substitution for Eu and Ce substitution for La result in a significant increase in the Eu and Ce average oxidation state due to the increased chemical pressure in the lattice. At the same time the Eu valence in $Pr_{0.8}Eu_{0.2}Co_2P_2$ deviates significantly from +3, despite the similarity of structure to $PrCo_2P_2$ with the integer +3 valence of praseodymium and to the high-pressure form of $EuCo_2P_2$, also with the postulated +3 valence of europium [1]. The magnetic properties of $La_{1-x}Ce_xCo_2P_2$ are quite different from the case of structurally related compound $La_{1-x}Pr_xCo_2P_2$ at large Ce concentrations [9], i.e. exactly in samples with the largest deviation of Ce valence from +3. All these facts confirm the assumption [2] that the magnetic ordering in RCo_2P_2 systems is governed not only by the structural factors, but also by the electronic state of the rare-earth ion. In summary, the temperature and concentration dependences of Eu and Ce oxidation states and correlation with local interatomic distances can be formally associated with the hybridization between the partially localized $4f$-orbital of rare-earth and the $3d$-level of Co, which apparently is the reason for the modification of the long-range magnetic order.

Acknowledgments

This work is partially supported by RFBR (grant No. 11-02-01174-a) and NSF (DMR-0955353). Authors thank the HASYLAB program committee for providing the opportunity of RIXS and XAFS measurements (project No. I-20100397).

References

[1] Chefki M, Abd-Elmeguid M M, Micklitz H, Huhnt C, Schlabitz W, Reehuis M and Jeitschko W 1998 *Phys. Rev. Lett.* **80** 802–5
[2] Kovnir K, Reiff W M, Menushenkov A P, Yaroslavtsev A A, Chernikov R V and Shatruk M 2011 *Chem. Mater.* **23** 3021–24
[3] Kovnir K, Thompson C M, Zhou H D, Wiebe C R and Shatruk M 2010 *Chem. Mater.* **22** 1704–13
[4] Khomskii D I 1979 *Physics-Uspekhi* **129** 443–85
[5] Klementiev K V *XANES dactyloscope for Windows* freeware: www.cells.es/Beamlines/CLAESS/software/xanda.html
[6] Röhler J 1975 *J. Magn. Magn. Mater.* **47&48** 175–80
[7] Joly Y 2001 *Phys. Rev.* B **63** 125120-1-10
[8] Yaroslavtsev A A, Menushenkov A P, Chernikov R V *et al* 2012 *JETP Letters* **96** 44–48
[9] Menushenkov A P, Yaroslavtsev A A, Grishina O V *et al* 2012 *Solid State Phenom.* **190** 200–3